Microwave shielding with far-from-circular polarization

Tijs Karman [*]
ITAMP, Harvard-Smithsonian Center for Astrophysics, Cambridge, Massachusetts 02138, USA

(Received 16 December 2019; revised manuscript received 3 March 2020; accepted 10 March 2020; published 6 April 2020)

Ultracold polar molecules can be shielded from fast collisional losses using microwaves, but achieving the required polarization purity is technically challenging. Here, we propose a scheme for shielding using microwaves with polarization that is far from circular. The setup relies on a modest static electric field and is robust against imperfections in its orientation.

DOI: 10.1103/PhysRevA.101.042702

I. INTRODUCTION

Ultracold polar molecules are emerging as a platform for quantum science and technology with applications in precision measurement [1], quantum simulation [2–4], and computing [5–7]. Many species of ultracold molecules are now realized experimentally, either by associating ultracold atoms [8–14] or by directly cooling molecules [15,16]. The lifetime of ultracold molecules is limited by collisional losses [17–19], even at a typical molecular density of 10^{-10} cm^{-3}, which is orders of magnitude below that required for some applications. The collisional loss rates observed are of the order of the universal loss rate [20], suggesting that the loss occurs at short range when the molecules approach one another closely. For some molecules this short-range loss is attributed to two-body chemical reactions [21]. Nonreactive molecules undergo effective two-body loss at much the same rate, presumably mediated by the formation of long-lived collision complexes [22], which may subsequently be lost through three-body recombination [23] or photoinduced processes [24].

Collisional losses can be suppressed generally by inducing long-ranged repulsive interactions that prevent the molecules from reaching short range. This is referred to as shielding. The long-ranged interactions simultaneously lead to fast elastic scattering [25], potentially enabling evaporative cooling of ultracold molecules. Quéméner and Bohn have suggested electrostatic shielding of polar molecules in the $n = 1$ rotationally excited state [26]. This may require strong electric fields, of the order of $3.25b/\mu$ [27], where b is the rotational constant and μ the dipole moment. This requirement may be circumvented by microwave shielding [28], where ground-state molecules can be shielded by inducing repulsive resonant dipole-dipole interactions through microwave dressing with $n = 1$ rotationally excited states. Furthermore, Gorshkov *et al.* suggested using combined static and microwave fields to achieve shielding by a repulsive second-order interaction, after precisely canceling the first-order interactions due to both fields [29]. While microwave shielding is feasible in static fields, the mechanism was later shown to be different and not reliant on precise cancellation of first-order interactions [28].

The technically challenging requirement for implementing microwave shielding is realizing almost-pure circular polarization, especially in the presence of reflections of microwaves off the vacuum chamber. Microwave shielding is effective for circularly polarized microwaves [28] but not for linear polarization. The reason is that the coupling to the repulsive branch of the resonant dipole-dipole interaction, which provides shielding, depends on the orientation of polarization relative to the intermolecular axis [30]. In the case of linear polarization, collisions along the polarization direction are not shielded, while nonadiabatic transitions to lower field-dressed states lead to rapid loss. For circular polarization, collisions along all directions are shielded and nonadiabatic transitions are suppressed for sufficiently high Rabi frequencies. For elliptical polarization, nonadiabatic transitions cannot be fully suppressed, and effective shielding requires a polarization that is 90% circular in the field [30] or, equivalently, has a 20-dB power extinction ratio between σ^+ and σ^- components.

II. EXPERIMENTAL PROCEDURE

In this work, we propose a modified scheme for microwave shielding that is effective for polarizations that are far from circular. The main idea is illustrated in Fig. 1. General elliptical polarization can be characterized as

$$\begin{aligned}\sigma(\xi) &= \sigma_+ \cos\xi - \sigma_- \sin\xi \\ &= -[\sigma_x \sin(\xi + \pi/4) + i\sigma_y \cos(\xi + \pi/4)], \end{aligned} \quad (1)$$

which interpolates between σ_+ circular polarization at $\xi = 0$ and σ_x linear polarization at $\xi = \pi/4$. For ξ in this range, the semimajor and semiminor axes are along x and y. We then consider a transformation to a coordinate frame, $x'y'z'$, defined by a rotation about the semiminor axis, y, by an angle

$$\varphi = \mathrm{acos}[\cot(\xi + \pi/4)] \quad (2)$$

such that the polarization becomes $\sigma_{+'} \cos(\xi + \pi/4)\sqrt{2} + \sigma_{z'} \sin(\varphi) \sin(\xi + \pi/4)$. That is, any polarization can be thought of as being perfectly circular in the $x'y'$ plane and having an additional linear component along z'. Next, we

[*]tijs.karman@cfa.harvard.edu

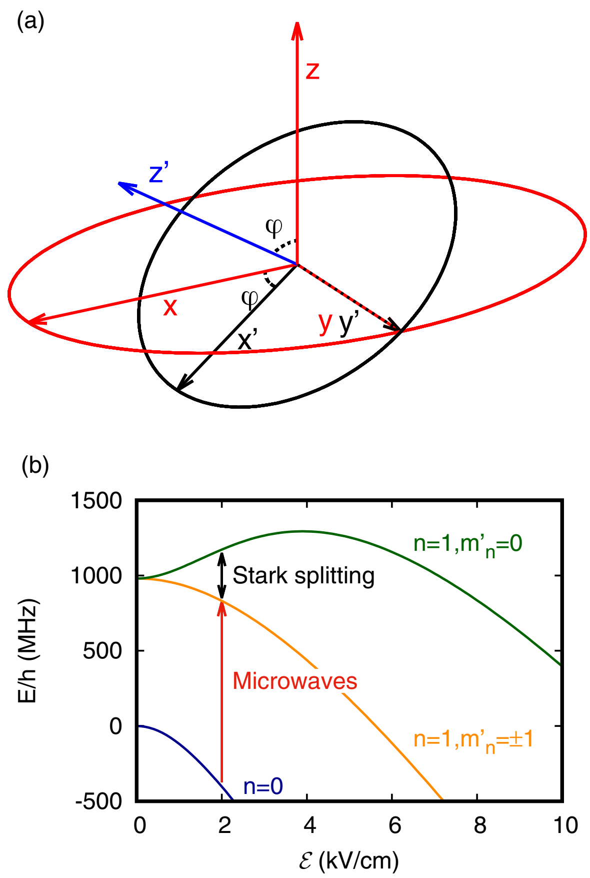

FIG. 1. (a) A general polarization ellipse where the x and y axes are chosen as the semimajor and semiminor axes is shown in red. This is equivalent to circular polarization in the $x'y'$ plane, shown in black, plus an additional linear polarization component along z', shown in blue. The coordinate transformation is discussed in the text. (b) A static $\mathcal{E}$ field along z' lifts the degeneracy of the $m_n' = 0$ and $m_n' = \pm 1$ states, such that the $n = 1$, $m_n' = 0$ state is Stark shifted out of resonance and the linear polarization component along z' has no effect. Under these conditions, the Hamiltonian reduces to that of polar molecules in the presence of circularly polarized microwaves and a static $\mathcal{E}$ field, which has previously been shown to realize effective shielding [28]. We note that the rotational angular momentum n is not strictly a good quantum number in an external $\mathcal{E}$ field, but rather it indicates the value of n that these states correlate with in the low-field limit.

consider applying a static $\mathcal{E}$ field along z', which lifts the degeneracy of the $m_n' = 0$ and $|m_n'| = 1$ states, where m_n' is the z' projection of the rotational angular momentum $\boldsymbol{n}$. This Stark shift serves to shift the $m_n' = 0$ state, addressed by the spurious $\sigma_{z'}$ polarization component, out of resonance, while the microwaves are kept tuned to the $m_n' = \pm 1$ states. Under these conditions, this Hamiltonian effectively reduces to dressing with microwaves that are purely circularly polarized about a static external field, which has previously been demonstrated to realize effective shielding [28].

We theoretically treat molecule-molecule collisions as in Refs. [28,30] and briefly summarize the approach here, whereas the relevant equations are given in the Appendix. The molecules are treated as rigid rotors that interact with one another through the dipole-dipole interaction and with static and ac electric fields through the Stark interaction. We then perform coupled-channel scattering calculations where at long range we match to the usual scattering boundary conditions, and at short range we match to a completely absorbing boundary condition [31], in the spirit of the universal loss model [20]. The short-range boundary condition is imposed at $R_{\rm min} = 20\ a_0$. The loss is insensitive to the precise value of $R_{\rm min}$ chosen, as shown in Ref. [28] The channel basis is truncated at $n_{\rm max} = 3$ and $L_{\rm max} = 6$. We distinguish between losses due to reaching short range (RSR) and microwave-induced loss (MIL). The latter corresponds to inelastic scattering into lower-lying field-dressed levels, which is referred to as MIL as these channels are not present in the absence of microwave radiation. It was found previously that microwave shielding requires strong dressing, $\Omega > \Delta$, and we here use resonant dressing, $\Delta = 0$, throughout. Experimental preparation of molecules in the upper field-dressed state on resonance can be achieved, for example, by adiabatically sweeping the microwave frequency from far blue detuned to resonance. The role of hyperfine degrees of freedom was addressed previously [28,30], and nuclear spin is not included here, as its effects can be suppressed by applying a modest magnetic field.

III. RESULTS AND DISCUSSION

Figure 2 shows the probability of the RSR and MIL rates for RbCs molecules at 1 μK as a function of the Rabi frequency, Ω, and static field strength, $\mathcal{E}$. This is obtained on resonance, $\Delta = 0$, and for a fixed ellipticity, $\xi = \pi/8$, which is halfway between σ_+ circular polarization at $\xi = 0$ and σ_x linear polarization at $\xi = \pi/4$. The static field is applied along the z' axis, i.e., between the polarization ellipse's normal and semimajor axis at an angle φ [see Eq. (2)]. At low field strengths, shielding is ineffective because the polarization is far from circular. At high field strengths, dipolar scattering becomes dominant and leads to high loss rates. At intermediate field strengths, there exists a region where losses due to RSR and MIL are small simultaneously, and effective shielding is realized. Shielding at higher Rabi frequencies, Ω, requires larger Stark splittings and hence field strengths, $\mathcal{E}$, leading to the triangular shape of the shielded region in Fig. 2. Shielding of losses to 2×10^{-13} cm^3 s—three orders of magnitude below the universal loss rate of 1.7×10^{-10} cm^3 s—is obtained for Rabi frequencies around $\Omega = 10$ MHz and field strengths around $\mathcal{E} = 1$ kV/cm.

Figure 3 shows the total loss rate, due to both RSR and MIL, as a function of the Rabi frequency, Ω, and microwave polarization ellipticity, ξ. Figures 3(a) and 3(b) correspond to static field strengths of $\mathcal{E} = 0$ and $\mathcal{E} = 1$ kV/cm, respectively. The static field is applied along the z' axis, which again lies at an angle φ [see Eq. (2)] between the polarization ellipse's normal and semimajor axis. At zero static field, shown in Fig. 3(a), shielding is effective only for polarizations that are close to circular, $4\xi/\pi < 0.1$, which corresponds to a power extinction ratio of the σ_- and σ_+ microwave field components larger than 22 dB [30]. For an achievable [11,32–34] field strength of $\mathcal{E} = 1$ kV/cm, shown in Fig. 3(b), effective shielding can be obtained for polarizations that are far from circular, with an eccentricity of up to $4\xi/\pi \approx 0.8$.

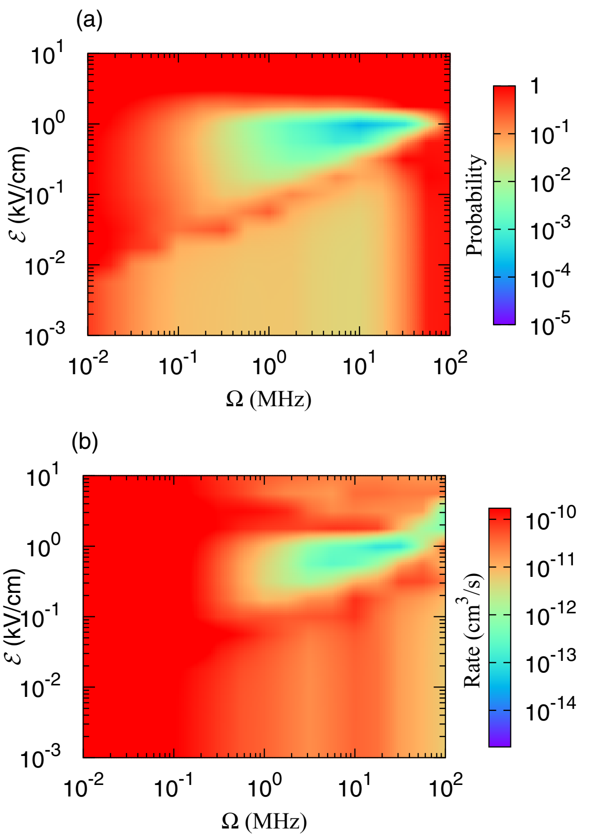

FIG. 2. Probability of the (a) RSR and (b) MIL rates as a function of Ω and the static field strength $\mathcal{E}$ for $\xi = \pi/8$, i.e., halfway between σ^+ and linear σ_x polarization. For high enough Ω values and intermediate field strengths, losses due to RSR and MIL are simultaneously small, and good shielding is obtained. A larger Stark splitting is required for increasing Rabi frequency, resulting in the triangle-shaped region of effective shielding. The loss rate due to RSR can be read from (a) using the intensity scale in (b).

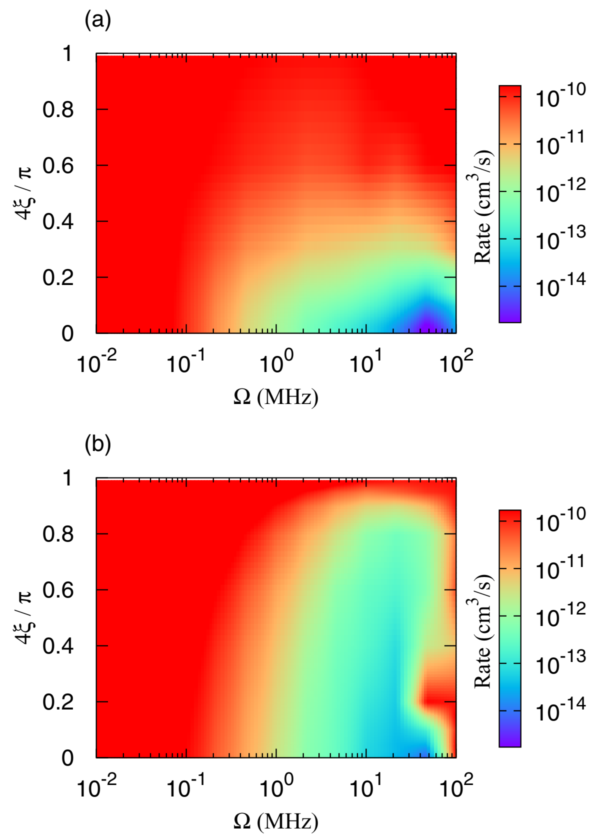

FIG. 3. Total loss rate due to both RSR and MIL as a function of Ω and ξ for (a) $\mathcal{E} = 0$ and (b) $\mathcal{E} = 1$ kV/cm. At zero field, shielding requires $4\xi/\pi \leqslant 0.1$, i.e., an imperfection in the ellipticity angle of less than 10%. Including a static field along z' enables shielding by elliptically polarized microwaves with a large eccentricity, up to $4\xi/\pi \approx 0.8$.

So far we have demonstrated that excellent shielding can be recovered for microwave polarizations that are far from circular by applying a static field exactly along z', which lies between the polarization ellipse's normal and semimajor axis. Next, we investigate the robustness of this scheme to imperfections in the alignment of $\boldsymbol{\mathcal{E}}$ and z'. Their alignment can be achieved by controlling the static field [34] or the microwave polarization [35], whichever is more practical. Figure 4 shows the total loss rate due to both RSR and MIL as a function of the undesired x' and y' components of the $\mathcal{E}$ field. Figure 4(a) shows loss rates for $4\xi/\pi = 3/4$, which corresponds to 25% σ_+ circular and 75% σ_x linear polarization. Even though the polarization ellipse is very eccentric and closer to being linear than it is to being circular, shielding of losses to below 10^{-12} cm^3 s can be achieved and requires alignment of the static field $\boldsymbol{\mathcal{E}}$ and the z' direction only to within 5°. Orientation of a static $\mathcal{E}$ field to this precision is feasible [34]. Figure 4(b) shows loss rates for $4\xi/\pi = 1/2$, which is halfway between circular and linear polarization and still too far from circular to realize shielding without the additional static field proposed here. In this case, the tolerances upon alignment of $\mathcal{E}$ and z' are even more forgiving, exceeding 10° for shielding of losses to below 10^{-12} cm^3 s.

IV. CONCLUSION

In conclusion, we have proposed a modified scheme for microwave shielding that is robust against large imperfections in the circular polarization, which is otherwise the main technical challenge for the experimental realization of microwave shielding. The main idea is that polarization imperfections can generally be regarded as a spurious linear polarization component perpendicular to a perfectly circular polarization. Application of a static field tunes the $m_n' = 0$ component, addressed by the spurious linear polarization component, out of resonance with the microwaves. The feasibility of the proposed scheme is illustrated by coupled-channel scattering calculations for bosonic RbCs molecules at 1 μK, for which we recover effective shielding with achievable static field strengths, $\mathcal{E} = 1$ kV/cm, and microwave Rabi frequencies, $\Omega = 10$ MHz, even for polarizations that are far from circular. Furthermore, the proposed scheme is robust against imperfections in the relative orientation of the polarization and static field. The tolerance of their misalignment may exceed 10°, depending on the eccentricity of the polarization.

ACKNOWLEDGMENTS

Discussions with J. Covey, Z. Yan, and M. Zwierlein regarding the experimental feasibility are gratefully

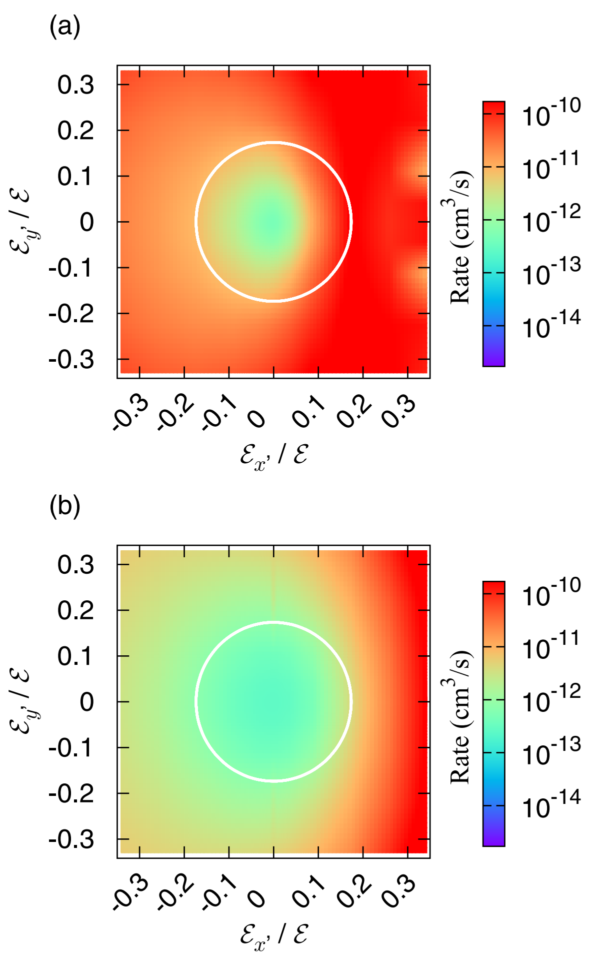

FIG. 4. Total loss rate due to RSR and MIL as a function of $\mathcal{E}_{x'}$ and $\mathcal{E}_{y'}$ imperfections in the orientation of an $\mathcal{E} = 1$ kV/cm static field. (a) $4\xi/\pi = 3/4$ and (b) $4\xi/\pi = 1/2$. These polarizations can be thought of as 25% and 50% circular, respectively. In both cases, the polarization ellipse is too eccentric to provide shielding without the additional static field. The white circle indicates an imperfection in the orientation of the static field of 10°. Shielding of losses below 10^{-12} cm^3 s for $4\xi/\pi = 3/4$ requires orienting $\mathcal{E}$ along z' to within 5°, and the tolerance is even more forgiving for polarizations that are closer to circular.

acknowledged. This work was supported by NWO Rubicon Grant No. 019.172EN.007 and the National Science Foundation through ITAMP.

APPENDIX: FORMALISM

The molecules are modeled as rigid rotors with a dipole moment,

$$\hat{H}^{(X)} = b_{\text{rot}}\hat{n}^2 - \hat{\mu}^{(X)} \cdot \vec{E}_{\text{static}} + \hat{H}_{\text{ac}}^{(X)}, \tag{A1}$$

with rotational constant b_{rot}. The second term, the Stark interaction with the static field, is described in more detail below. The last term represents the interaction with a microwave field [36],

$$\hat{H}_{\text{ac}}^{(X)} = -\sqrt{\frac{\hbar\omega}{2\epsilon_0 V_0}}\left[\hat{\mu}_\sigma^{(X)}\hat{a}_\sigma + \hat{\mu}_\sigma^{(X)\dagger}\hat{a}_\sigma^\dagger\right] + \hbar\omega(\hat{a}_\sigma^\dagger\hat{a}_\sigma - N_0). \tag{A2}$$

Here, $N_0 = \epsilon_0 E_{\text{ac}}^2 V_0/2\hbar\omega$ is the reference number of photons in a reference volume, V_0, at microwave electric field strength, E_{ac} [37]. The operators $\hat{a}_\sigma^\dagger$ and $\hat{a}_\sigma$ are creation and annihilation operators for photons at angular frequency ω in polarization mode $\sigma(\xi) = \sigma_+ \cos\xi - \sigma_- \sin\xi$.

The total Hamiltonian is

$$\hat{H} = -\frac{\hbar^2}{2M}\frac{1}{R}\frac{d^2}{dR^2}R + \frac{\hbar^2\hat{L}^2}{2MR^2} + \hat{H}^{(A)} + \hat{H}^{(B)} + \hat{V}(R). \tag{A3}$$

Here M is the reduced mass, R is the intermolecular distance, and $\hat{L}$ is the angular momentum operator associated with the end-over-end rotation. The first and second terms describe the radial and centrifugal kinetic energy, respectively. The final term is the dipole-dipole interaction between the molecules [28].

We use the basis functions

$$|n_A m_A\rangle|n_B m_B\rangle|LM_L\rangle|N\rangle. \tag{A4}$$

Only even L are included and the basis functions are adapted to permutation symmetry [28]. Coupled-channel calculations are performed using the renormalized Numerov algorithm [38] with absorbing boundary conditions at short range [31]. The calculations are converged to a few percent accuracy while truncating the basis at $n_{\max} = 3$ and $L_{\max} = 6$, where a lower $n_{\max}$ is required at a lower static $\mathcal{E}$ field.

The second term in Eq. (A1) represents the Stark interaction with the static field, which is newly proposed here. The static field is given by

$$\boldsymbol{\mathcal{E}} = \begin{pmatrix} \cos\varphi & 0 & \sin\varphi \\ 0 & 1 & 0 \\ -\sin\varphi & 0 & \cos\varphi \end{pmatrix}\begin{pmatrix} \mathcal{E}_{x'} \\ \mathcal{E}_{y'} \\ \mathcal{E}_{z'} \end{pmatrix}, \tag{A5}$$

where φ is given by Eq. (2). The components $\mathcal{E}_{x'}$ and $\mathcal{E}_{y'}$ represent imperfections in the orientation of $\boldsymbol{\mathcal{E}}$.

Figure 5 shows adiabatic potential curves, defined as eigenvalues of the Hamiltonian, Eq. (A3), excluding the radial kinetic energy as a function of the intermolecular distance, R. These are shown for $\Omega = 10$ MHz and $\xi = \pi/8$, which is halfway between circular and linear polarization, and shielding is ineffective without the additional static field proposed here. The lowest initial adiabatic potential, i.e., correlating with both molecules in the upper field-dressed level, is highlighted in color for clarity. Figure 5(a) shows adiabatic potential curves for zero static field, $\mathcal{E} = 0$, where crossings with potential curves correlating with lower field-dressed levels occur near the zero of energy. Figure 5(b) shows adiabatic potential curves for $\mathcal{E} = 1$ kV/cm, where these curve crossings do not occur except at short R, where the potentials have become strongly repulsive. Figures 5(c) and 5(d) offer expanded views of the same potential curves. We note that

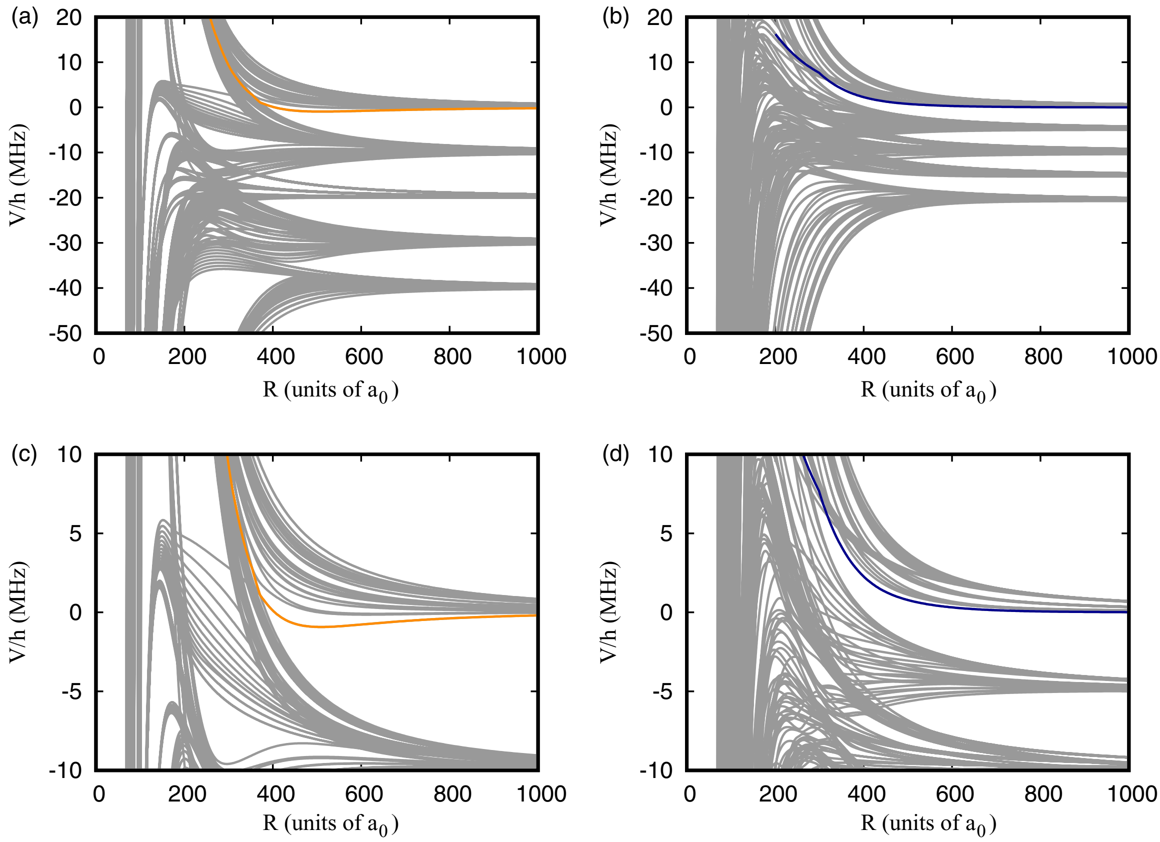

FIG. 5. Adiabatic potential curves for $\Omega = 10$ MHz and $\xi = \pi/8$. (a) $\mathcal{E} = 0$ and (b) $\mathcal{E} = 1$ kV/cm. (c, d) Expanded views. The lowest initial-state potentials are highlighted in color for clarity.

the static field polarizes the molecules in the absence of microwaves, and the resulting pendular states have a reduced effective Rabi coupling at a fixed microwave field strength, which is apparent from the smaller spacing of the asymptotic channels. As a result, shielding becomes ineffective at static field strengths that are too high (see Fig. 2).

[1] V. Andreev, D. G. Ang, D. DeMille *et al.* (ACME Collaboration), Nature **562**, 355 (2018).

[2] L. Santos, G. V. Shlyapnikov, P. Zoller, and M. Lewenstein, Phys. Rev. Lett. **85**, 1791 (2000).

[3] A. Micheli, G. K. Brennen, and P. Zoller, Nat. Phys. **2**, 341 (2006).

[4] M. A. Baranov, M. Dalmonte, G. Pupillo, and P. Zoller, Chem. Rev. **112**, 5012 (2012).

[5] D. DeMille, Phys. Rev. Lett. **88**, 067901 (2002).

[6] S. F. Yelin, K. Kirby, and R. Côté, Phys. Rev. A **74**, 050301(R) (2006).

[7] K.-K. Ni, T. Rosenband, and D. D. Grimes, Chem. Sci. **9**, 6830 (2018).

[8] K.-K. Ni, S. Ospelkaus, M. H. G. de Miranda, A. Pe'er, B. Neyenhuis, J. J. Zirbel, S. Kotochigova, P. S. Julienne, D. S. Jin, and J. Ye, Science **322**, 231 (2008).

[9] T. Takekoshi, L. Reichsöllner, A. Schindewolf, J. M. Hutson, C. R. Le Sueur, O. Dulieu, F. Ferlaino, R. Grimm, and H.-C. Nägerl, Phys. Rev. Lett. **113**, 205301 (2014).

[10] P. K. Molony, P. D. Gregory, Z. Ji, B. Lu, M. P. Köppinger, C. R. Le Sueur, C. L. Blackley, J. M. Hutson, and S. L. Cornish, Phys. Rev. Lett. **113**, 255301 (2014).

[11] J. W. Park, S. A. Will, and M. W. Zwierlein, Phys. Rev. Lett. **114**, 205302 (2015).

[12] M. Guo, B. Zhu, B. Lu, X. Ye, F. Wang, R. Vexiau, N. Bouloufa-Maafa, G. Quéméner, O. Dulieu, and D. Wang, Phys. Rev. Lett. **116**, 205303 (2016).

[13] T. M. Rvachov, H. Son, A. T. Sommer, S. Ebadi, J. J. Park, M. W. Zwierlein, W. Ketterle, and A. O. Jamison, Phys. Rev. Lett. **119**, 143001 (2017).

[14] A. Yang, S. Botsi, S. Kumar, S. B. Pal, M. M. Lam, I. Čepaitė, A. Laugharn, and K. Dieckmann, Phys. Rev. Lett. (to be published), arXiv:1908.02703.

[15] S. Truppe, H. J. Williams, M. Hambach, L. Caldwell, N. J. Fitch, E. A. Hinds, B. E. Sauer, and M. R. Tarbutt, Nat. Phys. **13**, 1173 (2017).

[16] D. J. McCarron, M. H. Steinecker, Y. Zhu, and D. DeMille, Phys. Rev. Lett. **121**, 013202 (2018).

[17] X. Ye, M. Guo, M. L. González-Martínez, G. Quéméner, and D. Wang, Sci. Adv. **4**, eaaq0083 (2018).

[18] M. Guo, X. Ye, J. He, M. L. González-Martínez, R. Vexiau, G. Quéméner, and D. Wang, Phys. Rev. X **8**, 041044 (2018).

[19] P. D. Gregory, M. D. Frye, J. A. Blackmore, E. M. Bridge, R. Sawant, J. M. Hutson, and S. L. Cornish, Nat. Commun. **10**, 3104 (2019).

[20] Z. Idziaszek and P. S. Julienne, Phys. Rev. Lett. **104**, 113202 (2010).

[21] S. Ospelkaus, K.-K. Ni, D. Wang, M. H. G. de Miranda, B. Neyenhuis, G. Quéméner, P. S. Julienne, J. L. Bohn, D. S. Jin, and J. Ye, Science **327**, 853 (2010).

[22] M. Mayle, B. P. Ruzic, and J. L. Bohn, Phys. Rev. A **85**, 062712 (2012).

[23] A. Christianen, T. Karman, and G. C. Groenenboom, Phys. Rev. A **100**, 032708 (2019).

[24] A. Christianen, M. W. Zwierlein, G. C. Groenenboom, and T. Karman, Phys. Rev. Lett. **123**, 123402 (2019).

[25] L. Lassablière and G. Quéméner, Phys. Rev. Lett. **121**, 163402 (2018).

[26] G. Quéméner and J. L. Bohn, Phys. Rev. A **93**, 012704 (2016).

[27] M. L. González-Martínez, J. L. Bohn, and G. Quéméner, Phys. Rev. A **96**, 032718 (2017).

[28] T. Karman and J. M. Hutson, Phys. Rev. Lett. **121**, 163401 (2018).

[29] A. V. Gorshkov, P. Rabl, G. Pupillo, A. Micheli, P. Zoller, M. D. Lukin, and H. P. Büchler, Phys. Rev. Lett. **101**, 073201 (2008).

[30] T. Karman and J. M. Hutson, Phys. Rev. A **100**, 052704 (2019).

[31] L. M. C. Janssen, A. van der Avoird, and G. C. Groenenboom, Phys. Rev. Lett. **110**, 063201 (2013).

[32] K.-K. Ni, S. Ospelkaus, D. J. Nesbitt, J. Ye, and D. S. Jin, Phys. Chem. Chem. Phys. **11**, 9626 (2009).

[33] K.-K. Ni, A Quantum Gas of Polar Molecules, Ph.D. thesis, Department of Physics, Faculty of the Graduate School of the University of Colorado, 2009.

[34] J. P. Covey, *Enhanced Optical and Electric Manipulation of a Quantum Gas of KRb Molecules* (Springer, Berlin, 2018).

[35] S. M. Bowers, A. Safaripour, and A. Hajimiri, IEEE J. Solid-State Circ. **50**, 1224 (2015).

[36] C. Cohen-Tannoudji, J. Dupont-Roc, and G. Grynberg, *Atom-Photon Interactions: Basic Processes and Applications* (Wiley, New York, 1998).

[37] A. V. Avdeenkov, New J. Phys. **17**, 045025 (2015).

[38] B. R. Johnson, J. Comput. Phys. **69**, 4678 (1978).